Generation and industrial applications of hollow light cylinders

Germán Da Costa*[a], José Cataldo[b], Rafael Guarga[b], Gabriel Usera[b] , Arturo Lezama[c] and Félix Mosqueda[a]

[a]Laboratorio de Optica y Fluidos, Departamento de Física, Univ. Simón Bolivar, A.P.89000, Caracas, Venezuela.

[b]Instituto de Mecánica de Fluidos, Facultad de Ingeniería, Montevideo, Uruguay.

[c]Instituto de Física, Facultad de Ingeniería, Montevideo, Uruguay.

ABSTRACT

A light beam structured as a hollow cone is obtained by oblique illumination of a cylindrical surface with a laser beam. The cylindrical surface may be a metallic needle or the core of an optical fiber. In the first case a speckle pattern appears around the light cone. The direction and mean length of light speckles are studied in the text. In the second case the light intensity distribution around the light cone presents bright and dark regions resulting from interference between light rays reflected from and passing through the fiber core. The hollow light cone is transformed into a hollow light cylinder (HLC) by means of a lens whose focus coincides with the cone vertex. The HLC is used to explore the cylindrical layer placed in the neighborhood of the internal wall of a combustion chamber model. Due to the large diameter of the model a Fresnel lens is used to transform the light cone into a light cylinder. This introduces additional optical noise in the system. The HLC is collected again by another Fresnel lens at the model output. A photodetector placed at the focus of the collected beam produces an electrical output showing pulses whenever residual particles pass through the explored region. A quantitative experimental analysis of the performance of the combustion chamber is thus performed.

Keywords: light cone, light cylinder, swirl flow, combustion chamber

1. INTRODUCTION

Properties of light cones obtained by oblique illumination of an optical fiber are studied in refs.(1,2). The light intensity distribution around the light cone presents bright and dark regions due to interference between light rays reflected at the fiber surface and light rays passing through the fiber. A light cone is also obtained by oblique illumination of a cylindric metallic needle with a laser beam. In that case the surface is opaque so there are no transmitted light rays. Therefore, periodic maxima and minima of light intensity are not present in the scattered light cone. But the light intensity distribution has the structure of a speckle pattern if the metallic needle surface is not perfectly smooth. In a preceding paper[3] the shape and dimensions of speckles obtained by normal illumination of a rough metallic cylinder were studied. In the present paper (Section 2) the study is extended to cover the case of an arbitrary angle between the cylinder and the laser beam, which is useful in any application related to Speckle Metrology[4-8] . It also allows us to generate hollow light cones in different kinds of optical setups with a thorough knowledge of their resulting optical properties. Moreover, the light cone is easily transformed into a hollow light cylinder by passing it through a lens. In Section 3 we analyze the performance of an industrial device where a hollow light cylinder is used to explore the region neighboring the internal wall of a torsional combustion chamber[9-13] , while general conclusions are presented in Section 4.

*Correspondence: E-mail: german@usb.ve

2. OPTICAL PROPERTIES OF HOLLOW LIGHT CONES

Fig.(1) shows a laser beam *(inc)* incident upon a circular cylindrical surface with radius (R). The angle between the laser beam and the cylinder axis (or a current generatrix, thus parallel to the axis, named "*g*" in fig.1) is (θ). The coordinate system (Oxyz) is so chosen that axis (Ox) coincides with the cylinder axis and the laser beam is parallel to plane (Oxy).

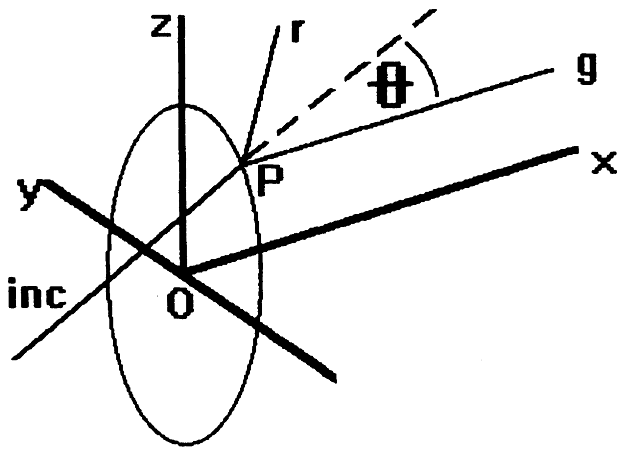

FIGURE 1

Consider the circular plane section of the cylinder with plane (Oyz). The position vector of a current point (P) and the normal unit vector of the circular plane section at point (P) are respectively:

$$\overline{OP} = R[0,-\cos(\Phi), sin(\Phi)] \qquad \text{(1a-c)}$$
$$\overline{n} = [0,-\cos(\Phi), sin(\Phi)]$$

where (Φ) is the angle between vector (OP) and the negative direction of axis (Oy). The unit vector of the incident laser beam is:

$$\overline{inc} = [\cos(\theta), sin(\theta), 0] \qquad (2)$$

Suppose that the surface of the cylinder is perfectly smooth. In that case the unit vector of the light ray reflected at point (P) ("*r*" in figs.1,2) is:

$$\overline{r} = \overline{inc} - 2(\overline{inc}.\overline{n})\overline{n} = [\cos(\theta), sin(\theta).\cos(2\Phi), sin(\theta).sin(2\Phi)] \qquad (3)$$

The intersection of the reflected light ray with an observation plane parallel to (Oyz) and abscissa (X) is a point (Q) (figs.2,3) with coordinates:

$$\overline{OQ} = [X, -R.\cos(\Phi) - X.tan(\theta).\cos(2\Phi), R.sin(\Phi) + X.tan(\theta).sin(2\Phi)] \qquad (4)$$

which reduces in the usual case $(X >> R)$ to:

$$\overline{OQ} = X.[1, -\cos(2\Phi) tan(\theta), sin(2\Phi) tan(\theta)] \qquad (5)$$

This shows (fig.3) that: a) point (Q) belongs to a circle with radius $X.tan(\theta)$ in the observation plane, and b) vector $O'\overline{Q}$ forms with the negative direction of axis (Oy) an angle (2Φ), while vector $O\overline{P}$ forms with the negative direction of axis (Oy) an angle (Φ). Therefore in the usual case where $(X >> R)$ and the laser beam diameter (D) is comparable to the cylinder diameter (that is $D \cong 2R$) the reflected light rays appear as coming from the vertex of a cone (fig.4) with axial symmetry around axis (Ox). Reflected light rays span the whole surface of the cone and they form an angle (θ) with its axis. The particular incident light ray which passes tangent to the cylinder belongs in fact to the family of reflected light rays. While the incident laser beam covers only half the cylindrical surface (for angle Φ determining the position of point P varies from $-\pi/2$ to $\pi/2$) the reflected beam covers a whole circle in the observation plane, for angle 2Φ determining the position of point Q varies from $-\pi$ to π.

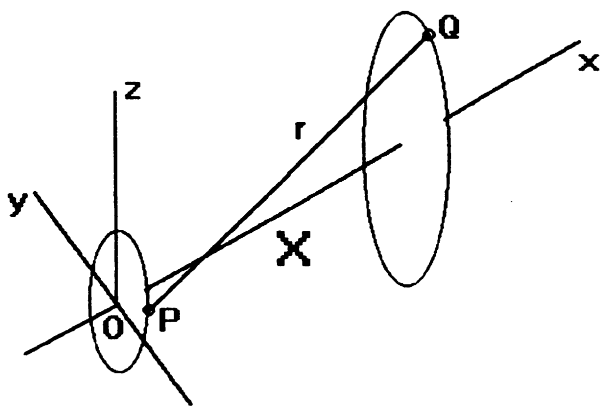

FIGURE 2

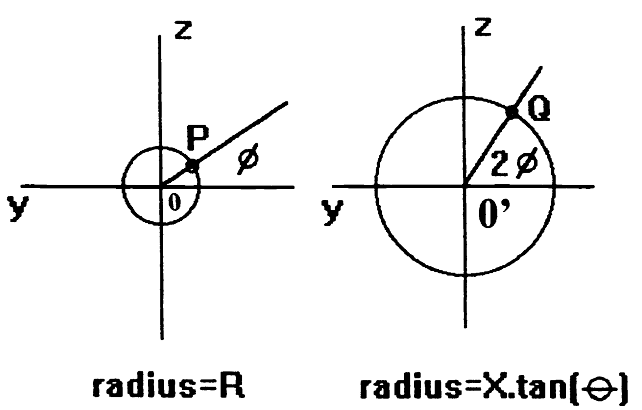

FIGURE 3

The preceding description is valid in the case when the cylinder surface is perfectly smooth. If the surface is smooth and transparent (for example, when the cylinder is the core of an optical fiber) we have in addition to the above considered reflected rays a family of transmitted light rays which pass through the fiber core and appear superimposed with the reflected rays in the observation plane. The reflected and transmitted rays span the same conical surface and give rise to maxima and minima of light intensity as a result of the difference in their optical paths[1,2] .

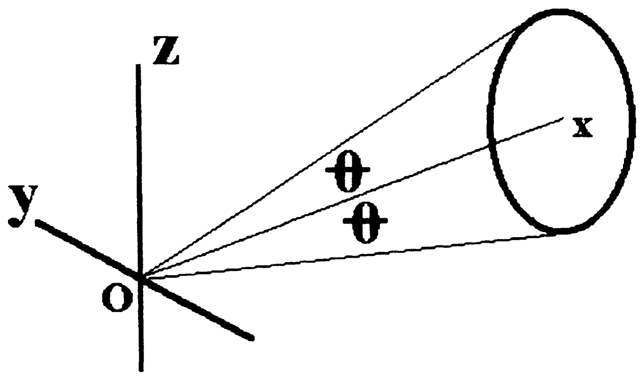

FIGURE 4

In the case when the surface is opaque and rough (for example when the scattering cylinder is a metallic needle) the properties of the scattered light field depend on the statistical properties of the surface roughness[4]. In what follows we make the hypothesis that light is scattered by the rough surface around point (P) within an angle (δ) centered in the reflected ray (r) calculated above (fig.5). Angle (δ) is supposed to depend not on the position of point (P) nor in the angle of incidence of the laser beam upon the scattering surface at point (P).

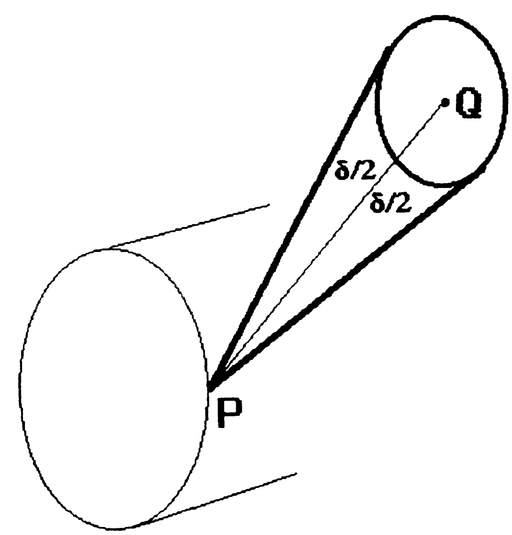

FIGURE 5

In other words, we assume that wavelets scattered from the neighborhood of a current point (P) fill the internal volume of a cone whose axis is the reflected ray (r) and such that the maximum angle between the wave vectors of scattered wavelets and the central ray *(r)* is $(\delta / 2)$. This problem was recently studied[3] in the special case when the laser beam is normal to the cylinder $(\theta = \pi/2\, radians)$. In the present paper the study is reduced to values of angle (θ) such that $\theta << 1$. As a result of scattering due to roughness the light intensity distribution around a current point (Q) in the observation plane is random and has the typical aspect of a laser speckle pattern[5]. The light field around point (Q) is due to contributions coming from points around (P) such as (A,B) in fig.6. Due to the limited angular extension of wavelets scattered from current points (A,B), if distance AB is too great the corresponding wavelets will not overlap at point (Q) (fig.7). The length of laser speckles appearing around (Q) is determined by the maximum distance between pairs of points around (P) such that the scattered wavelets partially overlap at (Q). This is a practical criterion used to determine the correlation length of speckles in a random light field issued from a rough surface[3,5]. This maximum distance, as well as the resulting length of light speckles, is calculated in what follows assuming that $\theta << 1$. The reason for this limitation is that for small values of angle (θ) the cone shown in fig.(5) intersects the observation plane approximately within a circle with radius $X.tan(\delta/2)$. This fact greatly simplify forecoming calculations. Of course, for an arbitrary value of angle (θ) the above cited intersection is an ellipse. Suppose now (fig.6) two points (A,B) placed symmetrically with respect to point (P) and such that vectors (OA, OB) form with vector (OP) the same angle $(\delta/4)$. Then the corresponding cones scattered from (A,B) intersect the observation plane approximately following two circles (fig.7) tangent at a point placed near point (Q) and centered at points (A′,B′) such that vectors (O′A′, O′B′) form with vector (OQ) an angle $(\delta/2)$.

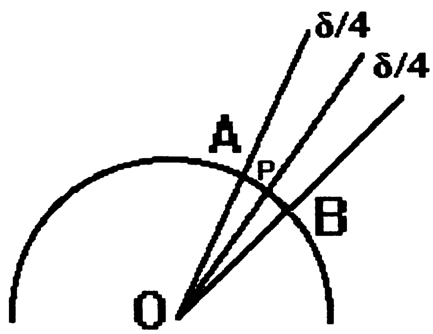

FIGURE 6

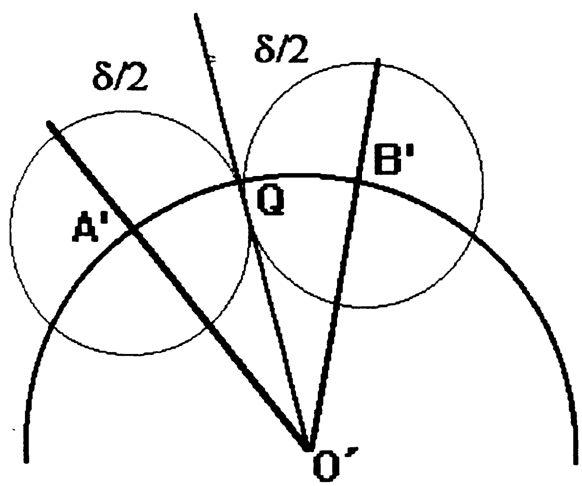

FIGURE 7

The resulting distance between points (A,B):

$$\overline{AB}_{max} = 2R.sin(\delta/4) \tag{6}$$

is the maximum allowed distance between points (A,B) such that wavelets issued from their neighborhood and due to surface roughness still appear superimposed at point (Q) in the observation plane. Superposition of scattered wavelets gives rise to a speckle pattern in the neighborhood of point (Q). In a hypothetical Young experiment having (A,B) as point sources an interference pattern is formed in the observation plane. The Young interference pattern contains bright and dark fringes normal to segment $(\overline{AB})$. The fringe width is $\lambda.X/\overline{AB}$, (λ) being the wavelength of the laser beam. The distance from the point sources (A,B) to the observation point is approximately equal to (X) in the hypothesis $(\theta << 1)$ made above. As the line tangent at point (Q) to the circle with radius $X.tan(\theta)$ (appearing in figs.2,3,5,7) is inclined at an angle $(\pi/2 - \Phi)$ with respect to the interference fringes, the distance between adjacent light intensity maxima observed along the line tangent at (Q) is $\lambda.X/\overline{AB}.\cos(\Phi)$. This distance is a minimum when $\overline{AB} = \overline{AB}_{max}$ (eq.6). Therefore the speckle correlation length in the neighborhood of point (Q) and along the direction tangent to the circle containing (Q) is:

$$w = \frac{\lambda.X}{AB_{max}.\cos(\Phi)} = \frac{\lambda.X}{2R.sin(\delta/4).\cos(\Phi)} \qquad (7)$$

The preceding formula gives, within the limits of validity of hypothesis stated above. an approximate value for the length of laser speckles in the direction tangent to the circle passing by point (Q) in the observation plane. As $0 \leq |\Phi| \leq \pi/2$ the length of tangent laser speckles around the circle in the observation plane varies from infinite in the prolongation of the incident laser beam to $\lambda.X/2Rsin(\delta/4)$ at the opposite region in the circle. Fig. (8) shows results of an experiment where the intensity distribution of light issued from a rough cylindrical needle is recorded with a CCD camera at different angular positions along a cross section of the scattered light cone. The closed curves appearing in the picture are loci of equal light intensity calculated and depicted by means of *Mathematica 3.0* software. They represent the laser speckles appearing around the circle. Their mean length in the direction tangential to the circle is an increasing function of their angular position, in coincidence with results of the preceding calculation. However, a precise numerical comparison between eq.(7) and the mean length of light speckles in fig.8 was not carried out and is a matter of current research. In fact. we remind that eq.7 is based on a particular hypothesis about the scattering law corresponding to the roughness distribution of the given surface. so that it does not have universal validity. Its functional dependence on angle (δ) must be reformulated in each particular case.

FIGURE 8

In applications described in the next Section a light beam structured as a hollow light cylinder is required. In that aim, the light cone generated in the preceding experiment is transformed into a light cylinder with the setup of fig. (9).

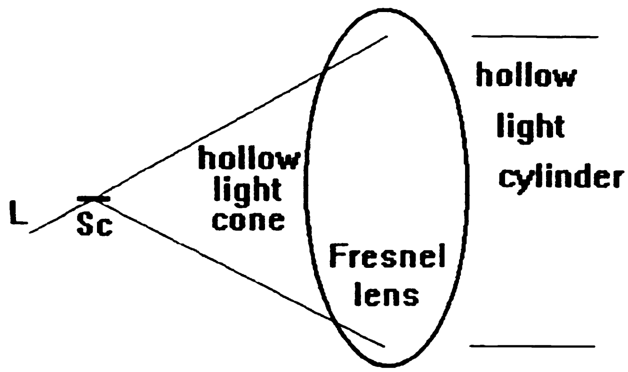

FIGURE 9

The cylindrical scattering element (Sc) is placed normal to a Fresnel lens and along its symmetry axis. The laser beam impinges the scattering element exactly at the focus of the Fresnel lens. In a typical experiment the diameter and focal distance of the lens are about 30cm and 20cm respectively. After passing through the lens the scattered light rays emerge as a hollow cylindrical light beam parallel to the lens symmetry axis. The optical quality of the light beam depends on the quality of the components of the optical system, that is the scattering element and the lens. In spite of their poor optical quality, Fresnel lenses are well adapted to this application because of their large diameter and small focal distance at a relatively low price. Negative photographs in fig.(10) show the light intensity distribution in a cross section of the light cylinder at two different distances (60cm in the left graph, 120cm in the right graph) from the Fresnel lens when the scattering element is an optical fiber. As the laser beam diameter (D) is greater than the scattering element diameter (2R) an intense light beam appears in the direction corresponding to $\Phi = \pi/2$, in the left side of each photograph. This beam is hidden by means of a dark stop.

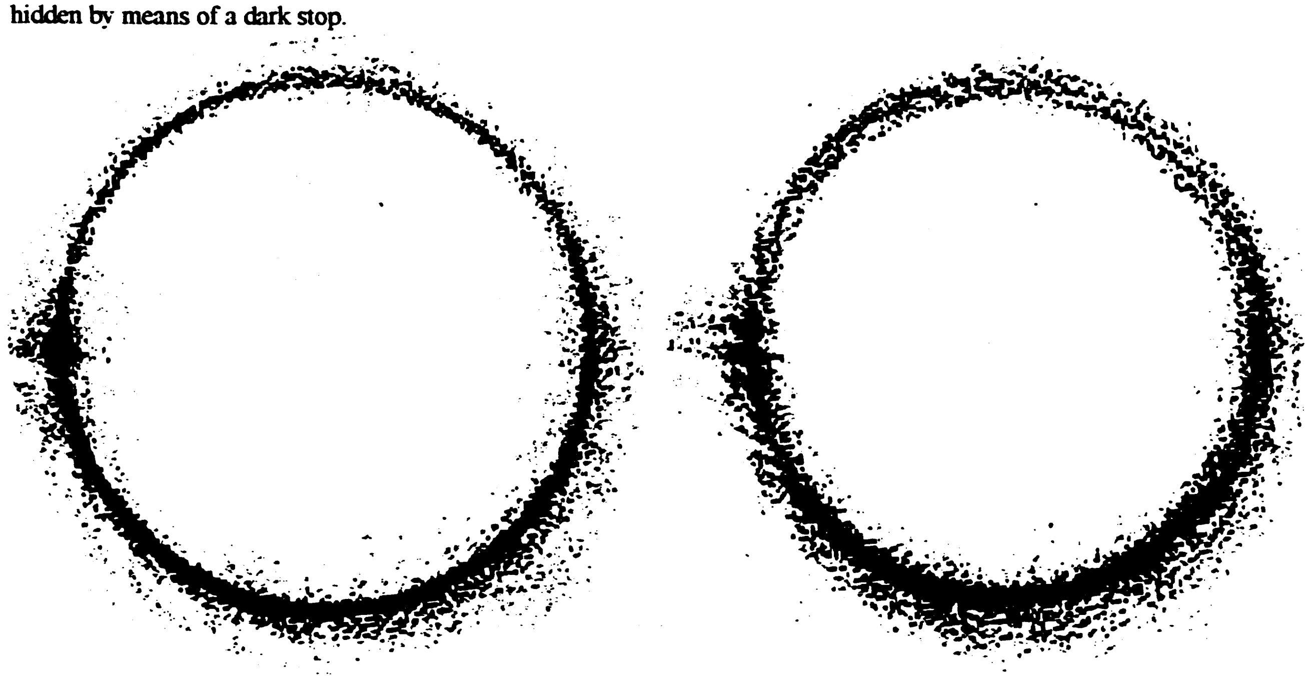

FIGURE 10

3. ANALYSIS OF PERFORMANCE OF COMBUSTION CHAMBERS USING LIGHT CYLINDERS

Metrological applications of speckle patterns scattered from cylindrical surfaces were recently developed[6-8]. In that case calculation of the direction and length of laser speckles presented in the preceding Section allows determination of the ultimate resolution of measurements. This interesting result is not exploited in the present paper. In what follows we rather present an industrial problem whose solution requires utilization of a light beam structured with the shape of a hollow light cylinder. Laser speckle is therefore a source of noise and should be avoided by using a scattering element as smooth as possible. This is an inconvenient of using a metallic needle as scattering element. On the other hand, we note that though an optical fiber core has a very smooth surface the scattered light cone presents maxima and minima of light intensity, which, as cited above, are due to interference between reflected and transmitted light rays. In the dark zones corresponding to light intensity minima the system is unable to detect the presence of intruder particles appearing in our actual application. The final decision on whether to use one or the other scattering element depends on the particular experiment conducted. In that sense the approximate though simple and intuitive result given by eq.7 is very useful to predict the behavior and optical properties of a given scattering element. Experiments are conducted at the Institute of Fluid Mechanics, Faculty of Engineering, Montevideo, Uruguay. In countries such as Uruguay, where fossil fuel wells are scarce and energetic requirements are ever increasing, a systematic effort is made in the aim of utilization of non-conventional fuels derived from industrial waste. This is the case of rice peel, which is specially difficult to handle because of its high content in silicates. Utilization of rice peel as fuel in conventional burners results in unacceptable erosion of the burner internal wall. Its low calorific power makes necessary a high residence time of the fuel within the combustion chamber, which in addition may be so shaped that a good mixture of air and fuel is assured. In the actual state of the art the so called Torsional Combustion Chamber (TCC) fulfills most of these requirements, except for problems derived from erosion. Essentially in a TCC the nozzles introducing air and fuel into the combustion chamber are placed around a circle and pointing in quasi-tangential directions, so that hot gas resulting from combustion follows an helicoidal flow pattern around the chamber symmetry axis[9-13]. Research efforts aim to keep solid residual ash far from the chamber internal wall in order to minimize erosion. The flow resulting of combustion is of course highly turbulent, which makes its analytical study very difficult. The main underlying idea to minimize erosion is to design the chamber shape and admission nozzles directions so that a high pressure region is established in the neighborhood of the wall. This gives rise to a "repellent layer" which rejects particles approaching the wall toward the chamber symmetry axis. In practice a trial and error design procedure is followed which combines analytical calculation and optical visualization of the resulting flow in a prototype chamber with transparent walls made in Plexiglas. As the critical region in the neighborhood of the chamber wall has the shape of a thin cylindrical layer, its optical exploration requires utilization of a light beam structured as a hollow cylinder. The experimental setup described in the preceding Section thus seems well adapted to this application. The complete setup used in the essays is shown in fig.(11). The relative positions of the laser beam (L), the scattering element (Sc) and Fresnel lens (Fr 1) as well as the diameter and focal length of the latter are so chosen that the diameter of the output light cylinder is slightly smaller than the diameter of the chamber internal wall. After passing through the combustion chamber model (CC) the light cylinder is focused again by means of another Fresnel lens (Fr 2). A photodetector (PD) is placed in the focus of the second lens. The voltage V(t) at the photodetector output is digitized and stored in a computer memory as a function of time. Therefore the optoelectronic system works as an "intruder detector" for particles approaching the chamber walls. Whenever a residual particle passes through the light cylinder a voltage pulse appears at the photodetector output. After processing the pulse sequence by software a statistical analysis of the frequency of appearance of particles in the forbidden region is performed. This yields a quantitative procedure for deciding whether or not the adopted design actually fulfills the imposed requirements.

Fig. 12 shows in detail the dimensions (in centimeters) and relative positions of the components of a typical model. Several similar models are used in the essays. From left to right, drawings in fig.12 represent respectively transverse and longitudinal sections of the model built in Plexiglas. The model is operated with air to simulate the true flow due to combustion. Air is blown by an external fan and enters into a large admission chamber (diameter 50cm in fig.12) where it is driven toward the main chamber (diameter 30 cm) by means of adjustable nozzles. As seen in fig.12, the length of the nozzles is 7cm and their mean inclination with respect to the chamber axis is 30 degrees. A CW, 17mW, HeNe laser beam was used to generate the hollow light cylinder. The photodetector (PD) output signal is digitized and stored by means of a Lab-PC+ card from National. The data acquisition system is controlled by LabWindows CVI software. The sampling frequency is 10^4 samples/second. A separate essay was conducted to determine the mean tangent and axial components of the air velocity vector at different radial positions. The velocity measurements are made using a directional Pitot tube. Typical results are shown in fig.13. This velocity pattern corresponds to a Rankine vortex associated with the swirl flow currently found in torsional combustion chambers[9-13]. Then the ability of the system to reject particles away from the chamber walls is analized by studying the PD output V(t) in the setup of fig.11. First the signal V(t) is recorded without particle injection. Even in the abscence of particles the output signal fluctuates around a mean value due to fluctuations in the air temperature and density which randomly deviate the light rays. Then polystyrene particles (density 29 gr/dm^3 and

47.3 gr/dm^3) are introduced at a bypass of the air injection system. A theoretical dimensional study was previously conducted in order to determine the convenient density and dimensions of injected particles which may better simulate the true combustion phenomenon. Figs.14-16 correspond to essays conducted in a small model with radius R=5cm. Fig.14 shows a typical PD output without particles in the upper graph and with particles in the lower graph. Though both signals have a random structure, the signal/noise ratio (dispersion of the statistical distribution of the output voltage divided by its mean value) is higher when particles are injected. The duration of each record is 1 second. The data acquisition system uses two channels and results are averaged in groups of 10 samples, so that (at a rate of 10^4 samples/second) records in fig.14 are taken at a rate of 500 averaged groups per second. This is the quantity recorded in the horizontal axis. Same convention is used in fig.15, where the PD output at different radial positions (named "r" , measured in centimeters and marked beside each graph) is shown. Figs.16(a,b) represent respectively the mean value and dispersion of the PD output at different radial positions. The horizontal axis represents the ratio between the actual radial coordinate and the chamber radius. Lectures in the vertical axis are respectively the actual mean value and dispersion divided by the mean value at r=0. The radial exploration is done by changing the diameter of the light cylinder. A clear advantage of the optical system used to generate the light cylinder is evident at this point. For the diameter of the light cylinder is easily changed just by adjusting the angle of incidence of the laser beam upon the optical fiber and without any further alteration of the setup.

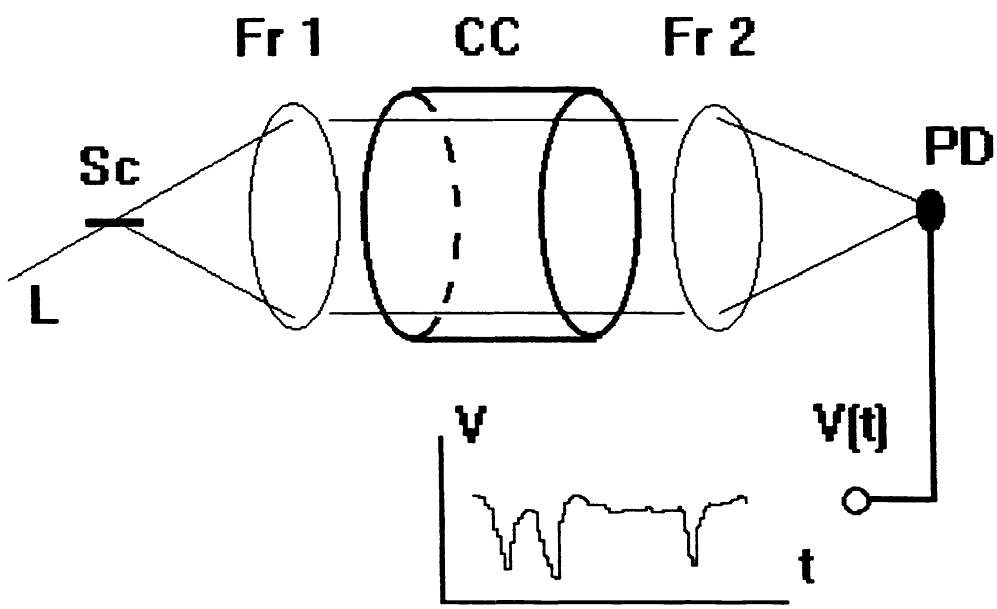

FIGURE 11

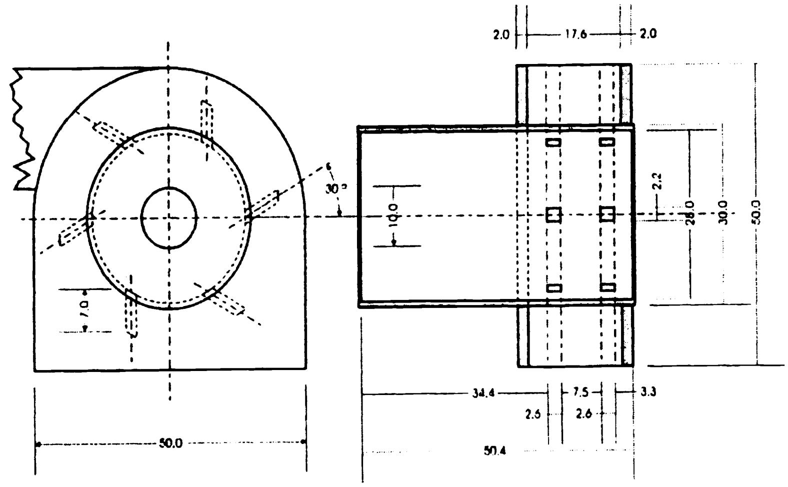
2.0
17.6
2.0
30°
10.0
7.0
2.2
28.0
30.0
50.0
50.0
34.4
7.5
3.3
2.5
2.6
50.4

FIG. 12

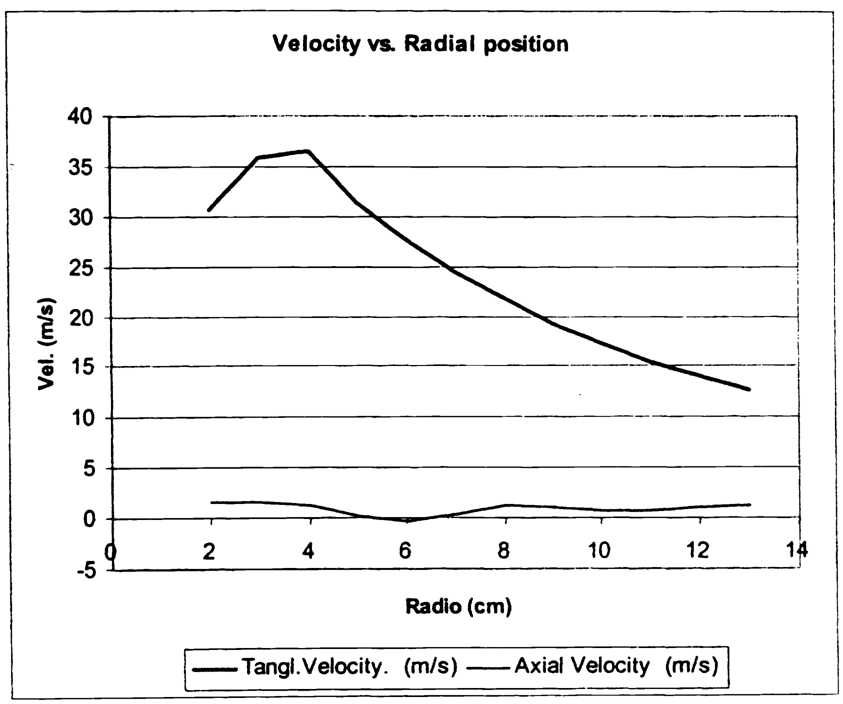
Velocity vs. Radial position
Vel. (m/s)
40
35
30
25
20
15
10
5
0
-5
0
2
4
6
8
10
12
14
Radio (cm)
Tangl.Velocity. (m/s)
Axial Velocity (m/s)

FIG. 13

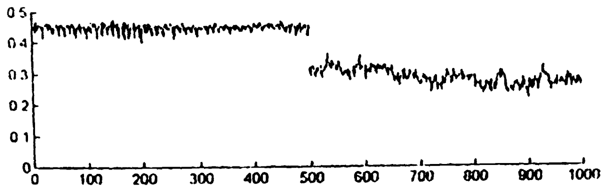

FIG. 14

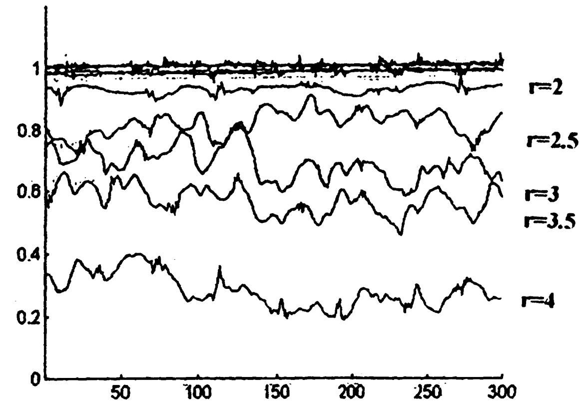

FIG. 15

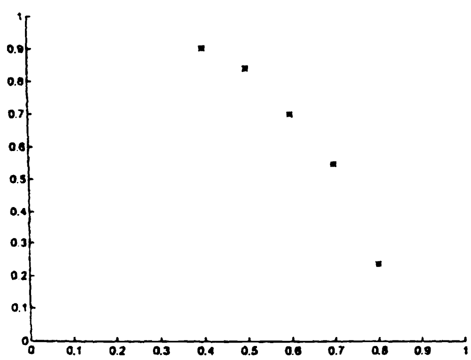

FIG. 16(a)

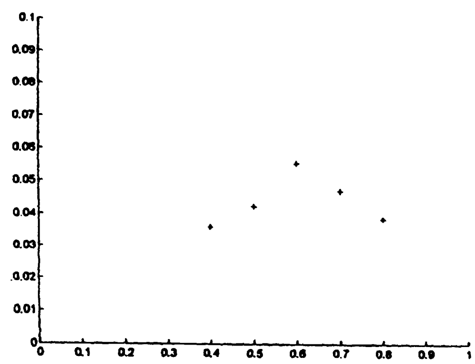

FIG. 16(b)

4. CONCLUSIONS

Basic optical properties of the field scattered by a rough cylindrical object obliquely illuminated by a laser beam were studied. The light field is formed by a hollow light cone surrounded by laser speckle. The correlation length of laser speckles in the direction tangent to a cross section of the light cone was calculated. The resulting equation (eq.7) is based on a simple hypothesis about the structure of light scattered from the rough surface, namely that the angular extension of the light field scattered from each point of the surface is independent: a)of the position of the considered point, and b) of the incidence angle of the laser beam upon the scattering surface at the considered point. In each particular case when this equation is applied the corresponding scattering law may be used. This result is useful whenever techniques derived from Speckle Metrology are applied to measure the displacements of rough cylindrical objects. In our actual case the light cone is transformed into a cylindrical hollow light beam by means of a Fresnel lens. The cylindrical beam is used to explore the neighborhood of the internal walls of a laboratory model of a combustion chamber. The optical quality of the cylindrical light beam is a decreasing function of the propagation distance. In our setup the length of the useful region where the optical quality of the light beam is acceptable is about 1 meter. The exploring beam is focused again after passing through a second Fresnel lens. The electrical output of a photodetector placed at the focal point is formed by a random sequence of pulses which correspond to the passage of residual combustion particles through the illuminated region near the chamber walls. Therefore the whole system works as an "intruder detector" where the forbidden region has the shape of a cylindrical layer. Statistical analysis of the output voltage yields numerical criteria for measuring the ability of the combustion chamber to keep the eroding residues far from the walls. As a final comment we note that the whole setup is robust, thus well adapted to work in an industrial environment, and makes use of standard optical components.

ACKNOWLEDGMENTS

The authors acknowledge financial support of National Research Councils of Uruguay and Venezuela, Faculty of Engineering (Uruguay) and Universidad Simón Bolivar (Venezuela).

REFERENCES

1. L.S. Watkins, "Scattering from side-illuminated clad glass fibers for determination of fiber parameters", J.Opt.Soc. Am. **64**, pp. 767-772, 1974.
2. Erna Frins, Horacio Failache, José Ferrari, Germán Da Costa and Arturo Lezama, " Optical fiber diameter determination by scattering at oblique incidence", Appl.Opt. **33**, pp. 7472-7476, 1994.
3. Germán Da Costa and José Ferrari, " Anisotropic speckle patterns in the light scattered by rough cylindrical surfaces", Appl.Opt. **36**, pp. 5231-5237, 1997.
4. J.M. Elson and J.M. Bennett, "Relation between the angular dependence of scattering and the statistical properties of optical surfaces", J.Opt.Soc.Am. **69**, pp. 31-47, 1979.
5. J.M. Burch and J.M. J. Tokarski, " Production of multiple beam fringes from photographic scatterers", Opt.Acta **15**, pp.101-111,1968.
6. I. Yamaguchi and T.Fujita, "Laser speckle rotary encoder", Appl.Opt. **28**, pp. 4401-4406 (1989)
7. M. Sjodahl and I.Yamaguchi, "Strain and torque measurements on cylindrical objects using the laser speckle strain gauge", Opt.Eng. **35**, pp. 1179-1186, 1996.
8. I.Yamaguchi, "Theory and applications of speckle displacement and decorrelation", in *Speckle Metrology*, R.S. Sirohi, ed. (Marcel Decker, New York, 1993) pp.1-39.
9. N.Syred and J.M. Beer, "Combustion in swirling flows: a review", Combustion and Flame **23**, pp. 143-201, 1974.
10. A.K. Gupta, D.G. Lilley and N. Syred, "Swirl flows" , Abacus Press, 1984.
11. J.K. Yoon and H.D. Shin, "Time-mean structures of the swirling flow with and without flame", J.Inst.Energy **60**, pp. 138-142, 1987.
12. S.A. Beltagui and N.R.L. Maccallum, "Characteristics of enclosed swirl flames with peripheral fuel injection", J.Inst.Energy **61**, pp. 3-16, 1988.
13. S.A. Beltagui, A.M.A. Kenbar and N.R.L. Maccallum, "Comparison of measured isothermal and combusting confined swirling flows- Peripheral fuel injection", Exp. Thermal and Fluid Science **6**, pp. 147-155, 1993.